

DIFFERENT GUARD INTERVAL TECHNIQUES FOR OFDM: PERFORMANCE COMPARISON

Heidi Steendam

TELIN Dept., Ghent University, Sint-Pietersnieuwstraat 41, 9000 GENT, BELGIUM

Heidi.Steendam@telin.UGent.be

Marc Moeneclaey

TELIN Dept., Ghent University, Sint-Pietersnieuwstraat 41, 9000 GENT, BELGIUM

Marc.Moeneclaey@telin.UGent.be

Abstract In this paper, we consider different types of guard intervals for OFDM systems, i.e. cyclic prefix (CP), zero padding (ZP) and known symbol padding (KSP). We compare the different OFDM systems with respect to their SNR performance. We show that CP-OFDM and ZP-OFDM have exactly the same performance, whereas KSP-OFDM has a slightly worse performance. Further, we consider data aided channel estimation for the three OFDM systems; the MSE of the estimators is compared to the corresponding Cramer-Rao bound. It turns out that in practice, channel estimation for CP-OFDM slightly outperforms the one for ZP-OFDM. The practical channel estimation techniques for KSP-OFDM perform worst.

Keywords: Guard intervals, ML channel estimation, Cramer-Rao bounds

1. Introduction

In multicarrier (MC) systems, where the data symbols are transmitted in parallel on N different carriers, the length T of a symbol is extended with a factor N [1]. This extension of the symbol length causes the MC system to be less sensitive to channel dispersion than a single carrier system transmitting data symbols at the same data rate. However, at the edges of a MC symbol, the channel dispersion still causes distortion, and hence introduces interference between successive MC symbols (i.e. intersymbol interference, ISI) and interference between different carriers within the same MC symbol (i.e. intercarrier interference, ICI). To reduce the effect of the ISI, each MC symbol is extended with a guard

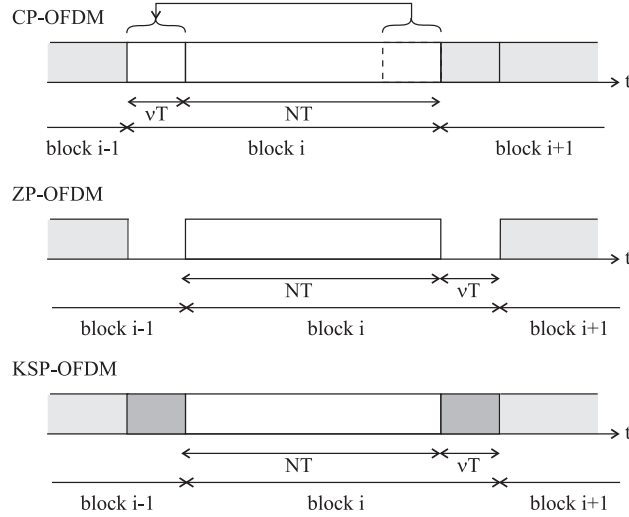


Figure 1. Transmitted signal for CP-OFDM, ZP-OFDM and KSP-OFDM.

interval. When the length of the guard interval is longer than the duration of the channel impulse response, ISI can completely be removed. However, as the transmission efficiency reduces with the insertion of the guard interval (during the guard interval, no new information can be transmitted), the guard interval must be chosen sufficiently small.

The most commonly used guard interval is the cyclic prefix (CP) [1]. In CP-OFDM, the last ν samples of each OFDM symbol of N samples are copied and added in front of the OFDM symbol, as shown in figure 1. At the receiver, the samples in the CP are discarded, as they are affected by interference; the N samples outside the CP are kept for further processing (see figure 2). Because during the guard interval signal is transmitted, the CP-OFDM system suffers from a power efficiency loss with a factor $\frac{N}{N+\nu}$. To avoid this power efficiency loss of CP-OFDM, the zero-padding guard interval was introduced [2]. In ZP-OFDM, a guard interval of ν samples is introduced after each OFDM symbol. During this guard interval, no signal is transmitted, as shown in figure 1. At the receiver, the ν samples of the guard interval are added to the first ν samples of the data part of N samples (see figure 2); the resulting N samples are then further processed by the receiver. Although the power efficiency loss is avoided in ZP-OFDM, we will show in the next section that the noise power will be enhanced with a factor $\frac{N+\nu}{N}$.

Another recently proposed guard interval is the known symbol padding (KSP) [3]-[4]. In KSP-OFDM, a guard interval consisting of ν known samples long is added after each OFDM symbol (corresponding to the

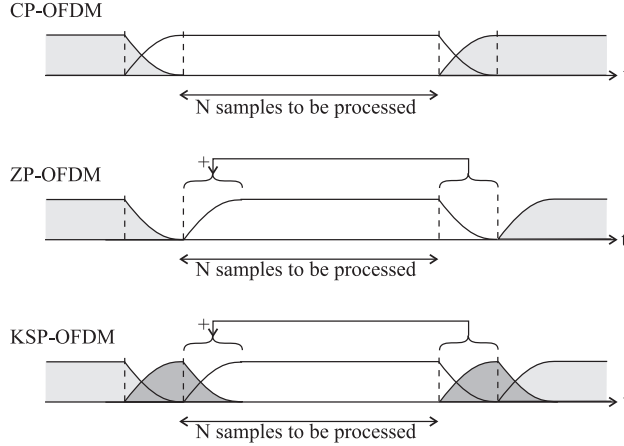


Figure 2. Received signal for CP-OFDM, ZP-OFDM and KSP-OFDM.

dark gray area in figure 1). Assuming the energy per sample is the same for the guard interval and the data part, KSP-OFDM will suffer, like CP-OFDM, from a power efficiency loss of $\frac{N}{N+\nu}$. At the receiver, first the signal corresponding to the known symbols is subtracted from the received signal (i.e. the dark gray areas in figure 2 are removed). Then, like in ZP-OFDM, the samples in the guard interval are added to the first part of the OFDM symbol, and the resulting N samples are further processed. Similarly to ZP-OFDM, KSP-OFDM will suffer from a noise power enhancement with a factor $\frac{N+\nu}{N}$.

The paper is organized as follows. In section 2, we will compare the SNR performance for the three OFDM systems. Then, in section 3, practical data-aided channel estimation techniques will be considered. The MSE performance of the estimators will be compared, and the corresponding Cramer-Rao lower bounds (CRLB) are derived. The conclusions will be drawn in section 4.

2. System Performance

2.1 CP-OFDM

The data symbols to be transmitted during the i th CP-OFDM block are defined as $\mathbf{a}_i = \{a_i(n) | n = 0, \dots, N - 1\}$. The data symbols are assumed to be statistically independent with $E[a_i(n)a_{i'}^*(n')] = E_s \delta_{i,i'} \delta_{n,n'}$. The data symbols are modulated on the carriers using an inverse fast Fourier transform (inverse FFT, IFFT), and the cyclic prefix is inserted.

The resulting samples transmitted during block i are given by

$$\mathbf{s}_{i,CP} = \sqrt{\frac{N}{N+\nu}} \mathbf{\Omega} \mathbf{F}^+ \mathbf{a}_i \quad (1)$$

where $\mathbf{s}_{i,CP} = \{s_{i,CP}(k) | k = -\nu, \dots, N-1\}$, \mathbf{F} is the $N \times N$ matrix corresponding to the FFT operation, i.e. $\mathbf{F}_{k,\ell} = \frac{1}{\sqrt{N}} e^{-j2\pi \frac{k\ell}{N}}$, and $\mathbf{\Omega}$ is the $(N+\nu) \times N$ matrix operator that adds the CP, i.e.

$$\mathbf{\Omega} = \begin{pmatrix} \mathbf{0}_{\nu \times (N-\nu)} & \mathbf{I}_\nu \\ & \mathbf{I}_N \end{pmatrix} \quad (2)$$

where $\mathbf{0}_{a \times b}$ is the $a \times b$ all-zero-matrix, \mathbf{I}_M is the $M \times M$ identity matrix and \mathbf{X}^+ is the Hermitian transpose of \mathbf{X} .

The time-domain samples (1) are transmitted over a doubly selective channel [5]. The channel is modeled as a tapped delay line with channel coefficients $h_{ch}(k; \ell)$. We assume that the channel contains a line-of-sight (LOS) component and a zero-mean multipath (MP) fading component, i.e. $h_{ch}(k; \ell) = h_{LOS}(k; \ell) + h_{MP}(k; \ell)$. The LOS component is modeled as $h_{LOS}(k; \ell) = \alpha e^{j\phi(\ell)} \delta(k)$, where the phase $\phi(\ell)$ depends on the time-selectivity of the channel, and the quasi-static amplitude α is assumed to be constant over a number of OFDM symbols. The channel taps of the multipath component are assumed to be WSSUS zero-mean Gaussian distributed [6] with autocorrelation function $R_{MP}(k; \ell)$

$$E[h_{MP}(k_1; \ell_1) h_{MP}^*(k_2; \ell_2)] = \delta(k_1 - k_2) R_{MP}(k_1; \ell_1 - \ell_2). \quad (3)$$

At the receiver, the CP is removed, and the remaining N samples are fed to the FFT. Without loss of generality, we consider the detection of the OFDM block with index $i = 0$. The N outputs of the FFT $y_{CP}(n)$ are given by $\mathbf{y}_{CP} = \sum_{i=-\infty}^{+\infty} \mathbf{F} \mathbf{\Delta} \mathbf{H}^{(i)} \mathbf{s}_{i,CP} + \mathbf{F} \mathbf{\Delta} \mathbf{w}$, where the $(N+\nu) \times (N+\nu)$ channel matrix $\mathbf{H}_{k,k'}^{(i)} = h_{ch}(k - k' - i(N+\nu); k)$, the operator $\mathbf{\Delta} = (\mathbf{0}_{N \times \nu} \quad \mathbf{I}_N)$ removes the prefix and $\mathbf{w} = \{w(k) | k = -\nu, \dots, N-1\}$ is the vector of time-domain noise samples. The noise components $w(k)$ are assumed to be statistically independent zero-mean Gaussian distributed with variance N_0 . The n th FFT output can be rewritten as

$$y_{CP}(n) = \sqrt{\frac{N}{N+\nu}} \sum_{i=-\infty}^{+\infty} \sum_{n'=-\nu}^{N-1} a_i(n') \gamma_{i,CP}(n, n') + W(n) \quad (4)$$

where $W(n) = (\mathbf{F} \mathbf{\Delta} \mathbf{w})_n$ and

$$\gamma_{i,CP}(n, n') = \frac{1}{N} \sum_{k=0}^{N-1} \sum_{k'=-\nu}^{N-1} h(k - k' - i(N+\nu); k) e^{-j2\pi \frac{kn - k'n'}{N}} \quad (5)$$

In [5] it is shown that the signal to interference and noise ratio (SINR) at the output of the FFT is independent of the carrier index n and is given by

$$SINR = \frac{\frac{N}{N+\nu} E_s P_U}{\frac{N}{N+\nu} E_s P_I + P_N} \quad (6)$$

where the contributions of the useful component, the interference and noise are given by

$$P_U = |\alpha|^2 |\Phi(0)|^2 + \frac{1}{N} \sum_{k=-\infty}^{+\infty} \sum_{\ell=-\infty}^{+\infty} \tilde{w}(k; \ell) R_{MP}(k; \ell) \quad (7)$$

$$P_I = |\alpha|^2 + \sum_{k=-\infty}^{+\infty} R_{MP}(k; 0) - P_U \quad (8)$$

$$P_N = N_0. \quad (9)$$

where $\Phi(n)$ is the n th output of the N -point FFT of the phase $\phi(\ell)$ and the weight function $\tilde{w}(k; \ell)$ is defined in [7, eq. A2].

2.2 ZP-OFDM

In ZP-OFDM, the data symbols \mathbf{a}_i are applied to the inverse FFT and zero padded, resulting in the time-domain samples

$$\mathbf{s}_{i,ZP} = \mathbf{\Xi} \mathbf{F}^+ \mathbf{a}_i \quad (10)$$

where the $(N + \nu) \times N$ matrix $\mathbf{\Xi} = (\mathbf{I}_N \quad \mathbf{0}_{N \times \nu})^T$ is the zero-padding operator and $\mathbf{s}_{i,ZP} = \{s_{i,ZP}(k) | k = 0, \dots, N + \nu - 1\}$. At the receiver, the guard interval samples are added to the first ν samples of the data part, and the resulting N samples are applied to the FFT. The N outputs $y_{ZP}(n)$ of the FFT can be written as $\mathbf{y}_{ZP} = \sum_{i=-\infty}^{+\infty} \mathbf{F} \mathbf{\Lambda} \mathbf{H}^{(i)} \mathbf{s}_{i,ZP} + \mathbf{F} \mathbf{\Lambda} \mathbf{w}$ where the $N \times (N + \nu)$ matrix $\mathbf{\Lambda}$ performs the addition of the guard interval to the data part

$$\mathbf{\Lambda} = \begin{pmatrix} \mathbf{I}_N & \mathbf{I}_\nu \\ \mathbf{0}_{(N-\nu) \times \nu} & \end{pmatrix} \quad (11)$$

The n th FFT output can be rewritten as

$$y_{ZP}(n) = \sum_{i=-\infty}^{+\infty} \sum_{n'=0}^{N-1} a_i(n') \gamma_{i,ZP}(n, n') + W(n) \quad (12)$$

where

$$\gamma_{i,ZP}(n, n') = \frac{1}{N} \sum_{k=0}^{N+\nu-1} \sum_{k'=0}^{N-1} h(k - k' - i(N + \nu); k) e^{-j2\pi \frac{kn - k'n'}{N}} \quad (13)$$

Using a similar analysis as for CP-OFDM in [5], it can be shown that the SINR at the FFT outputs for ZP-OFDM is independent of the carrier index n and yields

$$SINR = \frac{E_s P_U}{E_s P_I + P_N} \quad (14)$$

Although the summation ranges in (13) and (5) differ, it turns out that for ZP-OFDM P_U and P_I are the same as in CP-OFDM and are given by (7)-(8). The noise component $P_N = \frac{N+\nu}{N} N_0$, i.e. the noise power is enhanced with a factor $\frac{N+\nu}{N}$ as compared to CP-OFDM. Taking into account the effect of the power efficiency loss in CP-OFDM and the noise enhancement in ZP-OFDM, it follows that ZP-OFDM and CP-OFDM yield the same value of SINR.

2.3 KSP-OFDM

In KSP-OFDM, the time-domain samples to be transmitted are given by

$$\mathbf{s}_{i,KSP} = \sqrt{\frac{N}{N + \nu}} \begin{pmatrix} \mathbf{F}^+ \mathbf{a}_i \\ \mathbf{b}_g \end{pmatrix} \quad (15)$$

where it is assumed that the known symbols \mathbf{b}_g have the same energy per sample as the data samples, i.e. $E[|b_g(n)|^2] = E_s$. At the receiver, the signal corresponding to the known symbols \mathbf{b}_g is first subtracted from the received signal. After adding the ν samples of the guard interval to the data part of the OFDM symbol and applying the resulting N samples to the FFT, the FFT outputs are given by

$$\mathbf{y}_{KSP} = \sqrt{\frac{N}{N + \nu}} \sum_{i=-\infty}^{+\infty} \mathbf{F} \mathbf{\Lambda} \mathbf{H}^{(i)} \mathbf{\Xi} \mathbf{F}^+ \mathbf{a}_i + \mathbf{F} \mathbf{\Lambda} \mathbf{w} \quad (16)$$

where it is assumed that the channel taps are perfectly known, i.e. the contribution of the known symbols can completely be removed from the signal. Hence the outputs of the FFT for KSP-OFDM are the same as for ZP-OFDM, except for the power efficiency loss factor $\sqrt{\frac{N}{N+\nu}}$. The SINR at the outputs of the FFT is defined as (6), where the contributions P_U and P_I are given by (7)-(8), similarly as for CP-OFDM and ZP-OFDM, and the noise component $P_N = \frac{N+\nu}{N} N_0$ is the same as for ZP-OFDM. Comparing KSP-OFDM with CP-OFDM and ZP-OFDM, it

can be observed that KSP-OFDM will have worse performance than the two other systems, as it suffers from both power efficiency loss and noise enhancement, whereas CP-OFDM and ZP-OFDM suffer only from one of these effects. However, if the guard interval length is small as compared to the FFT length, as in most practical cases, the difference in performance will be very small. Further, in practical situations, the channel taps have to be estimated and are thus not perfectly known. In KSP-OFDM, the channel estimation error will cause interference from the known symbols, resulting in extra performance loss.

3. Channel Estimation

Reliable channel estimation is necessary in the above mentioned OFDM systems as data detection algorithms for these systems require the knowledge of the channel. Most common channel estimation techniques are data aided: pilot symbols are inserted in the OFDM signal to enable reliable detection of the channel. In this section, we will consider maximum-likelihood (ML) based data-aided channel estimation techniques for the three different OFDM systems, and compare the MSE of the channel estimation techniques. Further, we compare the performance of the estimators with the corresponding Cramer-Rao lower bounds.

In the following, we will assume that the channel changes slowly as compared to the duration of the length of an OFDM symbol, i.e. during the observed OFDM symbol, $h_{ch}(k; \ell) = h(k)$. We assume that the duration of the channel impulse response is L taps, and define the vector of channel taps $\mathbf{h} = (h(0) \dots h(L-1))^T$. To avoid intersymbol interference the duration of the guard interval exceeds the duration of the channel impulse response, i.e. $\nu \geq L - 1$.

In the following, we will show that for all cases, the observation can be written as $\mathbf{z} = \mathbf{D}\mathbf{h} + \boldsymbol{\omega}$, where the matrix \mathbf{D} depends on the inserted pilots and the noise $\boldsymbol{\omega}$ is zero-mean Gaussian distributed with autocorrelation function \mathbf{R}_ω , i.e. $\boldsymbol{\omega} \sim N(\mathbf{0}, \mathbf{R}_\omega)$. Hence, the observation \mathbf{z} given \mathbf{h} is Gaussian distributed: $\mathbf{z}|\mathbf{h} \sim N(\mathbf{D}\mathbf{h}, \mathbf{R}_\omega)$. The ML estimate of the vector \mathbf{h} is defined as [8]:

$$\hat{\mathbf{h}}_{ML} = \arg \max_{\mathbf{h}} p(\mathbf{z}|\mathbf{h}) \quad (17)$$

If \mathbf{R}_ω is independent of \mathbf{h} and $\mathbf{D}^+\mathbf{R}_\omega^{-1}\mathbf{D}$ is invertible, the ML estimate of the channel is given by

$$\hat{\mathbf{h}}_{ML} = (\mathbf{D}^+\mathbf{R}_\omega^{-1}\mathbf{D})^{-1}\mathbf{D}^+\mathbf{R}_\omega^{-1}\mathbf{z} \quad (18)$$

and the MSE of the estimation yields

$$MSE = E[||\mathbf{h} - \hat{\mathbf{h}}_{ML}||^2] = \text{trace}((\mathbf{D}^+\mathbf{R}_\omega^{-1}\mathbf{D})^{-1}) \quad (19)$$

The Cramer-Rao lower bound (CRLB) of the estimation is given by $\mathbf{R}_{\mathbf{h}-\hat{\mathbf{h}}} - \mathbf{J}^{-1} \geq 0$ [8] where $\mathbf{R}_{\mathbf{h}-\hat{\mathbf{h}}}$ is the autocorrelation matrix of the estimation error $\mathbf{h} - \hat{\mathbf{h}}$ and the Fisher information matrix \mathbf{J} is defined as

$$\mathbf{J} = E_{\mathbf{z}} \left[\left(\frac{\partial}{\partial \mathbf{h}} \ln p(\mathbf{z}|\mathbf{h}) \right)^+ \left(\frac{\partial}{\partial \mathbf{h}} \ln p(\mathbf{z}|\mathbf{h}) \right) \right] \quad (20)$$

Hence, the MSE is lower bounded by $E[|\mathbf{h} - \hat{\mathbf{h}}_{ML}|^2] = \text{trace}(\mathbf{R}_{\mathbf{h}-\hat{\mathbf{h}}}) \geq \text{trace}(\mathbf{J}^{-1})$. When equality occurs, i.e. when the MSE equals the CRLB, the estimate is a minimum variance unbiased (MVU) estimate. In the case that \mathbf{R}_{ω} is independent of \mathbf{h} , it can be shown that $\mathbf{J} = \mathbf{D}^+ \mathbf{R}_{\omega}^{-1} \mathbf{D}$, i.e. the channel estimate is a MVU estimate.

3.1 CP-OFDM

In CP-OFDM, data-aided channel estimation is performed by replacing some data carriers by pilot carriers. In this paper, without loss of generality, we consider the comb-type pilot arrangement [9], where in every OFDM symbol, $M \geq L$ data carriers are replaced by pilot carriers. The analysis however can easily be extended to other types of pilot arrangements.

Assuming that the pilot symbols $b_c(p)$ are located on carriers n_p , $p = 1, \dots, M$, it can be shown that the FFT outputs at positions n_p contain sufficient information for the ML estimation of the channel vector \mathbf{h} . Defining $z(p) = y_{CP}(n_p) / (\sqrt{\frac{N}{N+\nu}} b_c(p))$, the $M \times 1$ vector \mathbf{z} of observations can be written as $\mathbf{z} = \mathbf{A}\mathbf{h} + \mathbf{W}$, where the $M \times L$ matrix \mathbf{A} has entries $A_{k,\ell} = e^{-j2\pi \frac{n_k \ell}{N}}$, and the noise components \mathbf{W} are zero-mean Gaussian distributed with autocorrelation matrix $\mathbf{R}_{CP} = \frac{N+\nu}{N} \frac{N_0}{E_s} \mathbf{I}_M$. Hence, the observation \mathbf{z} given \mathbf{h} is Gaussian distributed: $\mathbf{z}|\mathbf{h} \sim N(\mathbf{A}\mathbf{h}, \mathbf{R})$. Taking into account that $\mathbf{A}^+ \mathbf{A}$ is invertible when $M \geq L$, it follows from (18) and (19) that $\hat{\mathbf{h}}_{ML} = (\mathbf{A}^+ \mathbf{A})^{-1} \mathbf{A}^+ \mathbf{z}$ and $MSE_{CP} = \frac{N+\nu}{N} \frac{N_0}{E_s} \text{trace}((\mathbf{A}^+ \mathbf{A})^{-1})$. When M divides N and the pilots are equally spaced over the carriers, i.e. $n_m = n_0 + (m-1) \frac{N}{M}$, it follows that $\text{trace}((\mathbf{A}^+ \mathbf{A})^{-1}) = \frac{L}{M}$, i.e. the MSE is proportional to the number of channel taps to be estimated, and inversely proportional to the number of pilots. As \mathbf{R}_{CP} is independent of \mathbf{h} , it follows that the ML estimate is MVU.

3.2 ZP-OFDM

Similarly as in CP-OFDM, data-aided channel estimation is performed by replacing some data carriers by pilot carriers. We consider the

same pilot arrangement as for CP-OFDM. As in CP-OFDM, it can be shown that the FFT outputs at the positions of the M pilots $b_c(p)$ contain sufficient information to perform the ML estimation. Defining $z(p) = y_{ZP}(n_p)/b_c(p)$, the observations can be written as $\mathbf{z} = \mathbf{A}\mathbf{h} + \tilde{\mathbf{W}}$, where \mathbf{A} is the same as for CP-OFDM and the noise contribution $\tilde{\mathbf{W}}$ is zero-mean Gaussian distributed with autocorrelation function $\mathbf{R}_{ZP} = \frac{N_0}{E_s} \mathbf{F}\mathbf{\Lambda}\mathbf{\Lambda}^+\mathbf{F}^+$, thus $\mathbf{z}|\mathbf{h} \sim N(\mathbf{A}\mathbf{h}, \mathbf{R}_{ZP})$. Hence, in the case that $\mathbf{A}^+\mathbf{R}_{ZP}^{-1}\mathbf{A}$ is invertible, the ML estimate of the channel is given by $\hat{\mathbf{h}}_{ML} = (\mathbf{A}^+\mathbf{R}_{ZP}^{-1}\mathbf{A})^{-1}\mathbf{A}^+\mathbf{R}_{ZP}^{-1}\mathbf{z}$ and the MSE of the estimation yields $MSE_{ZP} = \frac{N_0}{E_s} \text{trace}((\mathbf{A}^+\mathbf{R}_{ZP}^{-1}\mathbf{A})^{-1})$. Further, the ML estimate of the channel taps for ZP-OFDM is a MVU estimate, as \mathbf{R}_{ZP} is independent of \mathbf{h} .

3.3 KSP-OFDM

In the two previous techniques, we have assumed that there are M pilot symbols to estimate the L channel taps, $M \geq L$. In KSP-OFDM, the known symbols in the guard interval can be used as pilot symbols to estimate the channel. However, the guard interval contains only ν samples, with typically $\nu \approx L$. To increase the number of pilot symbols to M , we can consider two approaches: in the first approach, the guard interval length is kept to ν samples, and $M - \nu$ data carriers are replaced by pilot carriers. In the second approach, we increase the length of the guard interval to M samples, i.e. $\nu = M$.

Approach 1. As in the previous techniques, the comb-type pilot arrangement for the $M - \nu$ pilot carriers in the data part is considered. It can be shown that an observation interval corresponding to the $N + \nu$ time-domain samples of the i th OFDM block (as shown in figure 3) contains sufficient information for the estimation. Defining \mathbf{z} as the vector of $N + \nu$ observed samples, the observation can be written as $\mathbf{z} = \mathbf{B}\mathbf{h} + \boldsymbol{\epsilon}$ where $\mathbf{B} = \mathbf{B}_g + \mathbf{B}_c$ is a $(N + \nu) \times L$ matrix. The matrix \mathbf{B}_g corresponds to the contributions of the pilot symbols $b_g(p)$ in the guard interval with $(\mathbf{B}_g)_{i,j} = b_g(|i - j + \nu|_{N+\nu})$, $|x|_K$ is the modulo- K operation on x and $b_c(i) = 0$ for $i \geq \nu$ and $i < 0$. The matrix \mathbf{B}_c corresponds to the contributions of the pilot symbols $b_c(p)$ transmitted on the carriers with $(\mathbf{B}_c)_{i,j} = s_c(i - j)$; $\mathbf{s}_c = \mathbf{X}\mathbf{b}_c$ where the $N \times (M - \nu)$ matrix \mathbf{X} consists of the subset of columns of the IFFT matrix \mathbf{F}^+ corresponding to the positions of the pilot carriers, \mathbf{b}_c is the vector of the pilot symbols transmitted on the carriers, and $s_c(i) = 0$ for $i \geq N$ and $i < 0$, i.e. \mathbf{s}_c corresponds to the N -point IFFT of the pilot carriers only. Further, $\boldsymbol{\epsilon} = \mathbf{H}\mathbf{s}_d + \mathbf{w}$, where $(\mathbf{H})_{i,j} = h(i - j)$ is a $(N + \nu) \times N$ matrix, $\mathbf{s}_d = \bar{\mathbf{X}}\mathbf{a}$, \mathbf{a}

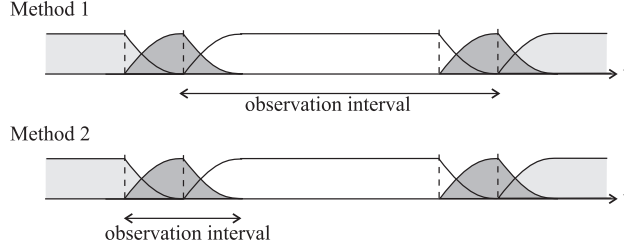


Figure 3. Observation interval for channel estimation in KSP-OFDM.

is the data vector, the $N \times (N - M + \nu)$ matrix $\bar{\mathbf{X}}$ consists of the subset of columns of the IFFT matrix \mathbf{F}^+ corresponding to the positions of the data carriers, i.e. \mathbf{s}_d corresponds to the N -point IFFT of the data carriers only, and \mathbf{w} is the additive Gaussian noise component. When $N - M + \nu$ is large, the data contribution $\mathbf{H}\mathbf{s}_d$ to ϵ can, according to the central limit theorem, be modeled as zero-mean Gaussian distributed. Hence, ϵ is zero-mean Gaussian distributed with autocorrelation matrix $\mathbf{R}_\epsilon = E_s \frac{N}{N+\nu} \frac{N+\nu-M}{N} \mathbf{H}\mathbf{H}^+ + N_0 \mathbf{I}_{N+\nu}$. As the autocorrelation matrix \mathbf{R}_ϵ depends on the parameters to be optimized, the ML estimator is very complex. In [4], a suboptimal ML-based solution is suggested: the autocorrelation matrix \mathbf{R}_ϵ is first estimated from the received signal, and the estimate $\hat{\mathbf{R}}_\epsilon$ is then used to find the estimate for \mathbf{h} :

$$\hat{\mathbf{h}}_{KSP,1a} = (\mathbf{B}^+ \hat{\mathbf{R}}_\epsilon^{-1} \mathbf{B})^{-1} \mathbf{B}^+ \hat{\mathbf{R}}_\epsilon^{-1} \mathbf{z} \quad (21)$$

where it is assumed that $\mathbf{B}^+ \hat{\mathbf{R}}_\epsilon^{-1} \mathbf{B}$ is invertible. To evaluate the performance of this estimate, we assume a genie-aided estimator for \mathbf{R}_ϵ , i.e. \mathbf{R}_ϵ is perfectly known. In this case, the MSE of the estimation of \mathbf{h} yields

$$MSE_{KSP,1a} = \text{trace}((\mathbf{B}^+ \mathbf{R}_\epsilon^{-1} \mathbf{B})^{-1}) \quad (22)$$

When \mathbf{R}_ϵ is not perfectly known, the MSE will be increased as compared to (22).

A disadvantage of the estimator (21) is that the autocorrelation matrix \mathbf{R}_ϵ needs to be known or estimated to be able to estimate the channel. As this autocorrelation matrix depends on the unknown channel, the estimation of this matrix from the received signal is not obvious. Therefore, a simplification of (21) can be made by ignoring the statistics of the interfering data, yielding the estimate

$$\hat{\mathbf{h}}_{KSP,1b} = (\mathbf{B}^+ \mathbf{B})^{-1} \mathbf{B}^+ \mathbf{z} \quad (23)$$

and the corresponding MSE is given by

$$MSE_{KSP,1b} = \text{trace}((\mathbf{B}^+ \mathbf{B})^{-1} \mathbf{B}^+ \mathbf{R}_\epsilon \mathbf{B} (\mathbf{B}^+ \mathbf{B})^{-1}) \quad (24)$$

As \mathbf{R}_ϵ depends on \mathbf{h} , also the CRLB is very complex. Therefore, we consider the low SNR limit of the CRLB. When E_s/N_0 is low, it can easily be verified that $\mathbf{R}_\epsilon \approx N_0\mathbf{I}_{N+\nu}$. In that case, the CRLB reduces to $E[\|\mathbf{h} - \hat{\mathbf{h}}_{ML}\|^2] \geq N_0\text{trace}((\mathbf{B}^+\mathbf{B})^{-1})$ i.e. for low SNR, the MSE's (22) and (24) of the estimates (21) and (23) reach the CRLB.

Approach 2. It can easily be verified that the observation interval shown in figure 3 contains sufficient information for the estimation in the second approach, where the pilot symbols are all located in the guard interval. The vector of $\nu + L - 1$ observed samples equals $\mathbf{z} = \mathbf{T}\mathbf{h} + \boldsymbol{\epsilon}'$ where $(\mathbf{T})_{i,j} = b_g(i-j)$ with $b_g(i)$ denoting the pilot symbols in the guard interval; note that $b_g(i) = 0$ for $i < 0$ or $i \geq \nu$. The noise component can be written as $\boldsymbol{\epsilon}' = \mathbf{H}^{(0)}\mathbf{s}_0 + \mathbf{H}^{(1)}\mathbf{s}_1 + \mathbf{w}$, where $\mathbf{s}_0 = (s_{0,KSP}(N-L+1) \dots s_{0,KSP}(N-1))^T$ and $\mathbf{s}_1 = (s_{1,KSP}(0) \dots s_{0,KSP}(L-2))^T$ are the contributions from the data parts of previous and next OFDM symbol, respectively, $(\mathbf{H}^{(0)})_{i,j} = h(L-1-(i-j))$ and $(\mathbf{H}^{(1)})_{i,j} = h(i-j-\nu)$ with $h(i) = 0$ for $i < 0$ and $i > L-1$. When N is large, \mathbf{s}_0 and \mathbf{s}_1 can be modeled as zero-mean Gaussian distributed. Hence, $\boldsymbol{\epsilon}' \sim N(\mathbf{0}, \mathbf{R}_{\epsilon'})$ with $\mathbf{R}_{\epsilon'} = E_s(\mathbf{H}^{(0)}(\mathbf{H}^{(0)})^+ + \mathbf{H}^{(1)}(\mathbf{H}^{(1)})^+) + N_0\mathbf{I}_{\nu+L-1}$. Similarly as for the first approach, the autocorrelation matrix $\mathbf{R}_{\epsilon'}$ depends on the parameters \mathbf{h} to be estimated. As in the previous method, a suboptimal ML based solution can be proposed [4] by assuming that the autocorrelation is first estimated from the received signal, and then used to estimate \mathbf{h} . The estimate $\hat{\mathbf{h}}_{KSP,2a}$ and the $MSE_{KSP,2a}$ (assuming $\mathbf{R}_{\epsilon'}$ is perfectly known) are then given by (21) and (22), where \mathbf{B} and \mathbf{R}_ϵ are replaced by \mathbf{T} and $\mathbf{R}_{\epsilon'}$, respectively.

As for the previous approach, the knowledge of $\mathbf{R}_{\epsilon'}$ is needed to estimate \mathbf{h} . To simplify the estimator, the statistics of the interfering data can be ignored. The resulting estimate $\hat{\mathbf{h}}_{KSP,2b}$ and the $MSE_{KSP,2b}$ are given by (23) and (24) by replacing \mathbf{B} and \mathbf{R}_ϵ by \mathbf{T} and $\mathbf{R}_{\epsilon'}$.

Further, similarly as for the first method, a low SNR limit for the CRLB can be found: $E[\|\mathbf{h} - \hat{\mathbf{h}}_{ML}\|^2] \geq N_0\text{trace}((\mathbf{T}^+\mathbf{T})^{-1})$. At low SNR, the MSE of the two estimates reach the CRLB.

3.4 Performance Comparison

In table 1, the energy per information data symbol $E_{s,i}$ and the bandwidth efficiency η_{BW} are given for the different guard interval techniques and pilot positions. When N is large, it is clear that the differences in $E_{s,i}$ and η_{BW} are small for the different techniques.

In figure 4, the normalized MSE, i.e. $NMSE = \frac{E_s}{N_0}MSE$, is shown as function of M for $N = 1024$, $L = 8$ and $\nu = 7$ (except for KSP2, where

	$E_{s,i}$	η_{BW}
CP-OFDM	$\frac{N+\nu}{N-M} E_s$	$\frac{N-M}{N+\nu} \frac{1}{T}$
ZP-OFDM	$\frac{N}{N-M} E_s$	$\frac{N+\nu}{N-M} \frac{1}{T}$
KSP1-OFDM	$\frac{N+\nu}{N+\nu-M} E_s$	$\frac{N+\nu-M}{N+\nu} \frac{1}{T}$
KSP2-OFDM	$\frac{N+\nu-M}{N} E_s$	$\frac{N}{N+M} \frac{1}{T}$

Table 1. Energy per information data symbol $E_{s,i}$ and bandwidth efficiency η_{BW} for the different guard interval techniques and pilot positions

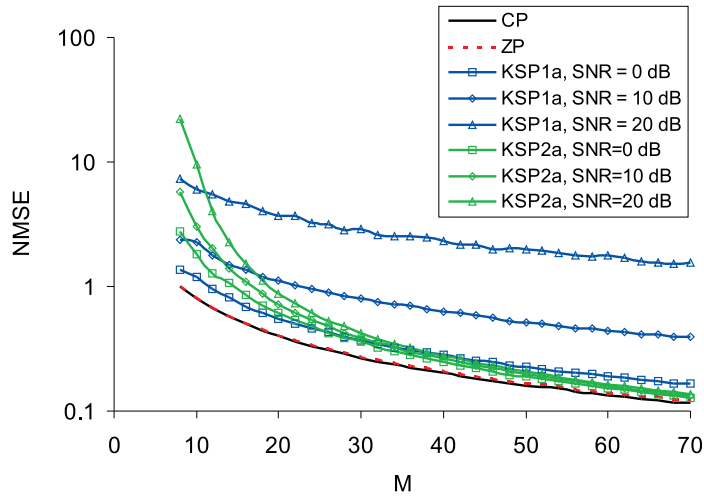


Figure 4. NMSE for $N = 1024$, $L = 8$, $\nu = 7$.

$\nu = M$). As can be observed, the MSE for CP-OFDM outperforms all other techniques. The MSE for ZP-OFDM however is very close to that of CP-OFDM: when $\nu \ll N$, the difference between channel estimation for CP-OFDM and ZP-OFDM will be very small. Further, it can be observed that the first method to estimate the channel in KSP-OFDM (KSP1), by adding pilots in the guard interval and on the carriers, has a much worse MSE performance than CP and ZP-OFDM, especially when the $SNR = \frac{E_s}{N_0}$ is increasing. Indeed, when SNR increases, the interference of the data symbols on the pilot symbols becomes more important, affecting the estimation of the channel. Also, the MSE for the second method for KSP-OFDM (KSP2) is shown. It follows from the figure that for increasing M , the MSE for KSP2 comes close to the ones for CP and ZP-OFDM, and is independent of the SNR. This can be explained as when the guard interval length increases, the relative importance of the interfering data symbols reduces.

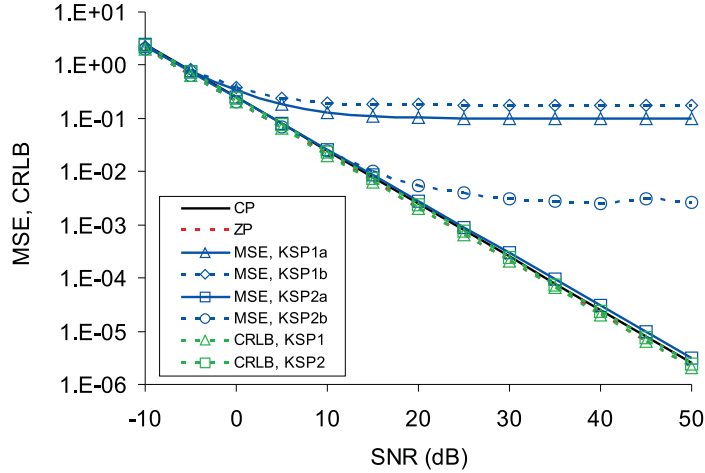


Figure 5. MSE and CRLB for $N = 1024$, $L = 8$, $\nu = 7$, $M = 40$.

In figure 5, the MSE and the CRLB are shown as function of the SNR for $N = 1024$, $L = 8$, $M = 40$ and $\nu = 7$ (except for KSP2, where $\nu = M$). It can be observed that the MSE for CP, OFDM and KSP2 almost coincide. The KSP1a technique performs worse than the three former techniques, especially at high SNR where the interference from the data symbols dominates: the MSE shows an error floor. Also in the KSP1b and KSP2b techniques, an error floor is present at high SNR: the estimates ignore the presence of the data symbols and at high SNR the data symbols are the dominant disturbance. The low SNR limit Cramer-Rao bounds for KSP1 and KSP2 are very close to each other and to the CRLBs of CP-OFDM and ZP-OFDM (which coincide with the MSE for these techniques).

4. Conclusions

In this paper, we have considered three guard interval techniques for OFDM systems, i.e. CP, ZP and KSP. First, we have compared the three techniques with respect to their SNR performance. It is shown that CP-OFDM and ZP-OFDM have the same SNR performance. The KSP-OFDM technique has a slightly worse performance, as it suffers from both power efficiency loss and noise enhancement, whereas the other two techniques suffer from only one of these effects.

Further, we have considered ML based channel estimation techniques for the three systems. We compared the MSE of the estimates with

the corresponding Cramer-Rao bounds. It turns out that CP-OFDM channel estimation outperforms the other techniques. However, the difference between the MSE performance of the ZP-OFDM technique and that of CP-OFDM is marginally small when $N \gg \nu$: i.e. ZP-OFDM and CP-OFDM have virtually the same MSE performance. KSP-OFDM has worse MSE performance than the other two techniques; the proposed KSP2 technique, where the guard interval length is extended, outperforms the KSP1 technique, where pilot symbols are placed in the guard interval and on carriers.

References

- [1] J. A. C. Bingham, "Multicarrier modulation for data transmission, an idea whose time has come," *IEEE Comm. Mag.*, Vol. 31, pp. 514, May 1990.
- [2] B. Muquet, Z. Wang, et. Al., "Cyclic Prefixing or Zero Padding for Wireless Multicarrier Transmissions?," *IEEE Trans. on Comm.*, Vol. 50, no 12, Dec 2002, pp. 2136-2148.
- [3] L. Deneire, B. Gyselinckx, M. Engels, "Training Sequence versus Cyclic Prefix – A New Look on Single Carrier Communication," *IEEE Comm. Letters*, Vol.5, no 7, Jul 2001, pp. 292-294.
- [4] O. Rousseaux, G. Leus, M. Moonen, "Estimation and Equalization of Doubly Selective Channels Using Known Symbol Padding," *IEEE Trans. on Signal Proc.*, Vol. 54, no 3, March 2006.
- [5] H. Steendam, "Multicarrier Parameter Optimization in Doubly-Selective Fading Channels with Line-of-sight Components," 9th Int. Symp. on Spread Spectrum Techniques and Applications, ISSSTA2006, Manaus, Brazil, August 2006.
- [6] R. Steele, *Mobile Radio Communications*. London, U.K.: Pentech, 1992.
- [7] H. Steendam, M. Moeneclaey, 'Analysis and Optimization of the Performance of OFDM on Frequency-Selective Time-Selective Fading Channels', *IEEE Trans. on Comm.*, Vol. 47, no 12, Dec 1999, pp. 1811-1819.
- [8] H.L. Van Trees, *Detection, Estimation and Modulation Theory*, New York, Wiley, 1968.
- [9] F. Tufvesson, T. Maseng, "Pilot Assisted Channel Estimation for OFDM in Mobile Cellular Systems," *Proc. of IEEE Veh. Tech. Conf., VTC'97*, Phoenix, U.S.A, May 4-7, 1997, pp. 1639-1643.